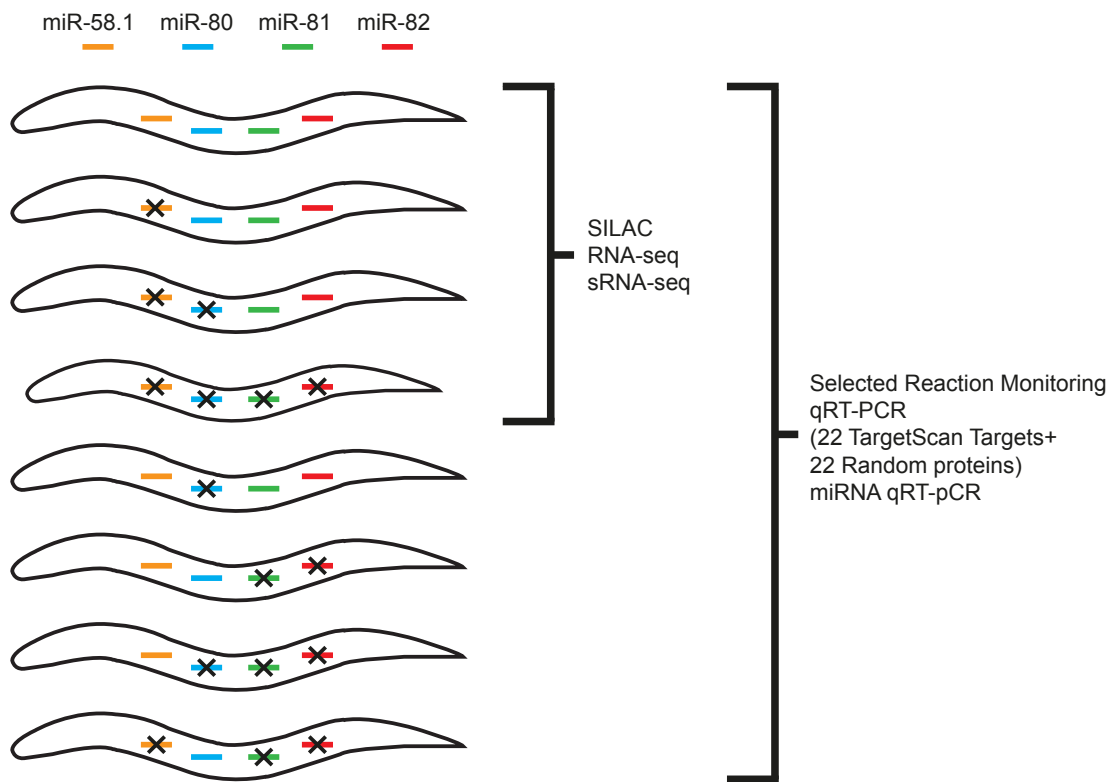


A**B**

C. elegans miR-58.1 UGAGAUCGUUCAGUACGGCAAU

C. elegans miR-80 UGAGAUCAUUAGUUGAAAGCCGA

C. elegans miR-81 UGAGAUCACGUGAAGCUAGU

C. elegans miR-82 UGAGAUCACGUGAAGCCAGU

C. elegans miR-58.2 AGAGAUCACCAUUGAGAUCCAA

C. elegans 2209.1 AGAGAUCAGCGGUUACACUACA

D. melanogaster bantam UGAGAUCAUUUUGAAGCUGAUU

Figure S1: Experimental overview and miR-58 family sequences.

A, Overview of experimental methods used to explore target regulation and redundancy of miR-58 family members. B, Sequences of the six *C. elegans* miR-58 family members and the *Drosophila melanogaster* bantam homologue. Conserved nucleotides that occur in half, or more than half, of the miR-58 family members are highlighted in black.

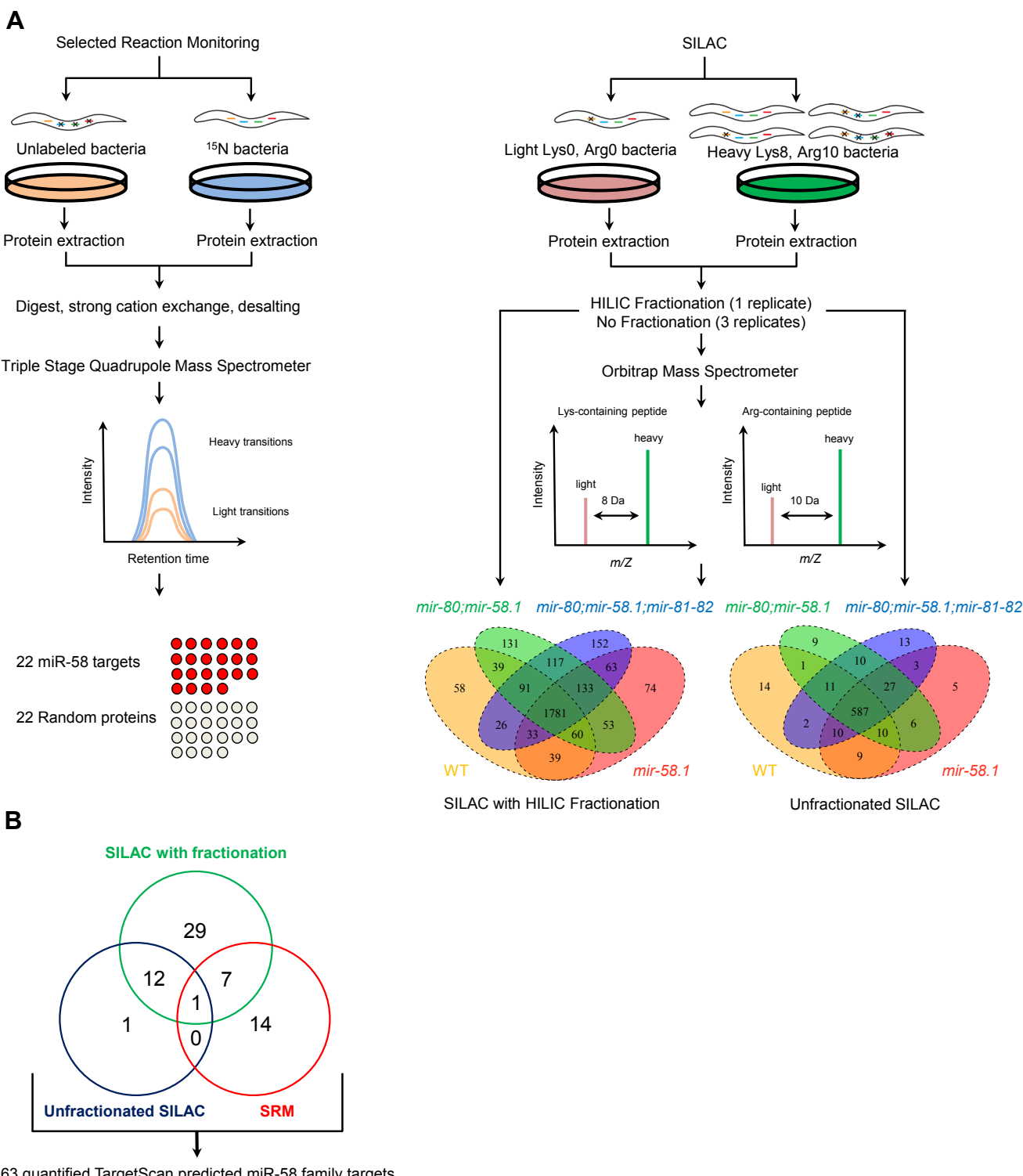


Figure S2: Combined Selected Reaction Monitoring (SRM) and SILAC approach quantified 63 TargetScan predicted miR-58 family targets.

A, Experimental outline of used targeted and shotgun proteomics to quantify protein abundance of miR-58 family targets. Selected reaction monitoring was used to quantify 22 miR-58 TargetScan predicted targets and a control group of 22 random proteins in all possible combinations of the three available miR-58 family deletions: *mir-58.1*, *mir-80* and *mir-81-82*. SILAC approach was used to quantify protein changes in 4 genetic backgrounds: WT (wild-type), *mir-58.1*, *mir-80*; *mir-58.1* and *mir-80*; *mir-58.1*; *mir-81-82*. SILAC experiments were performed in 2 variants: with HILIC fractionation and without. Unfractionated SILAC identified 587 overlapping proteins across 3 replicates. Fractionated SILAC identified 1781 overlapping proteins in 1 measured replicate. B, Overlap of quantified TargetScan predicted miR-58 family targets identified by selected reaction monitoring, SILAC with fractionation and unfractionated SILAC.

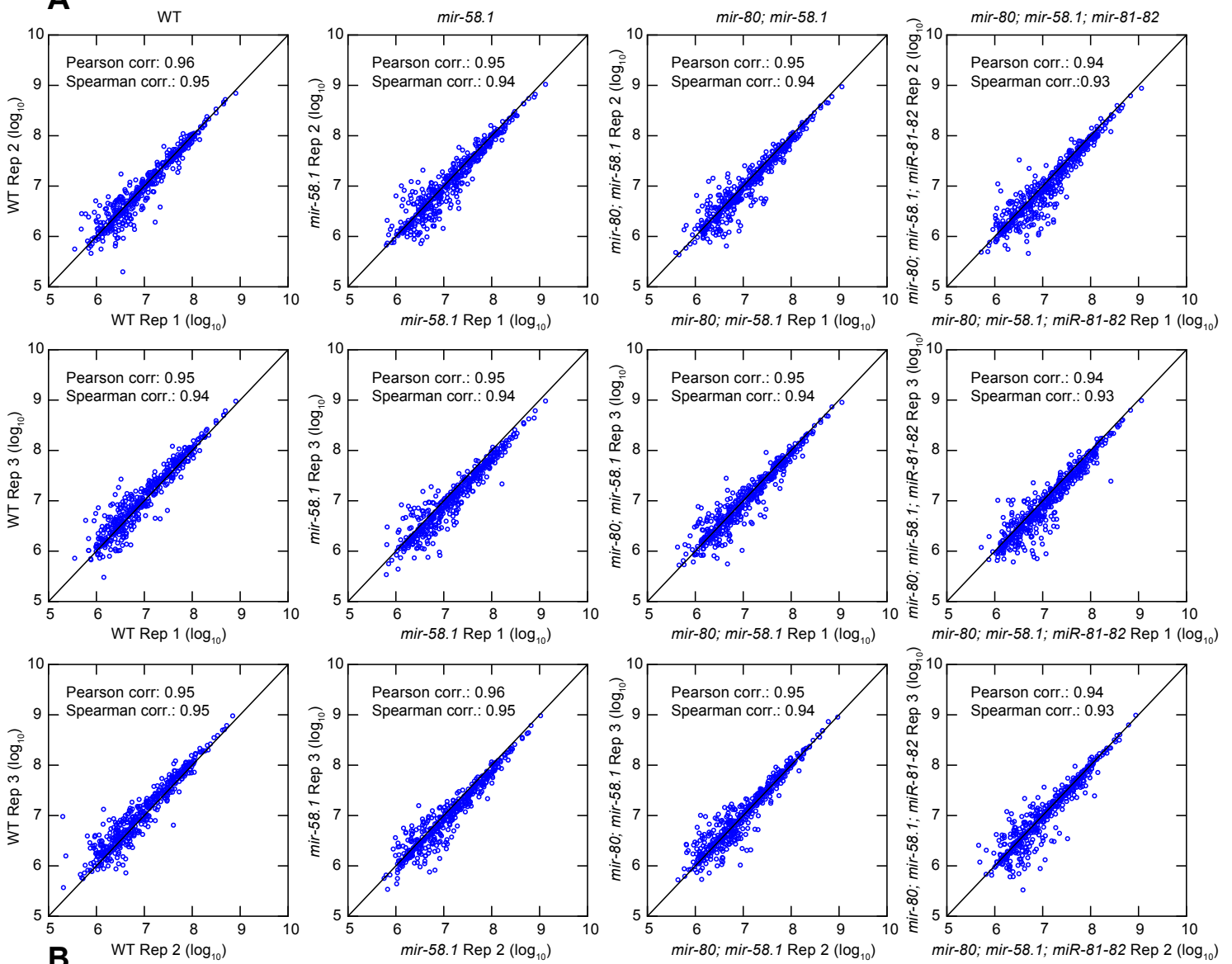
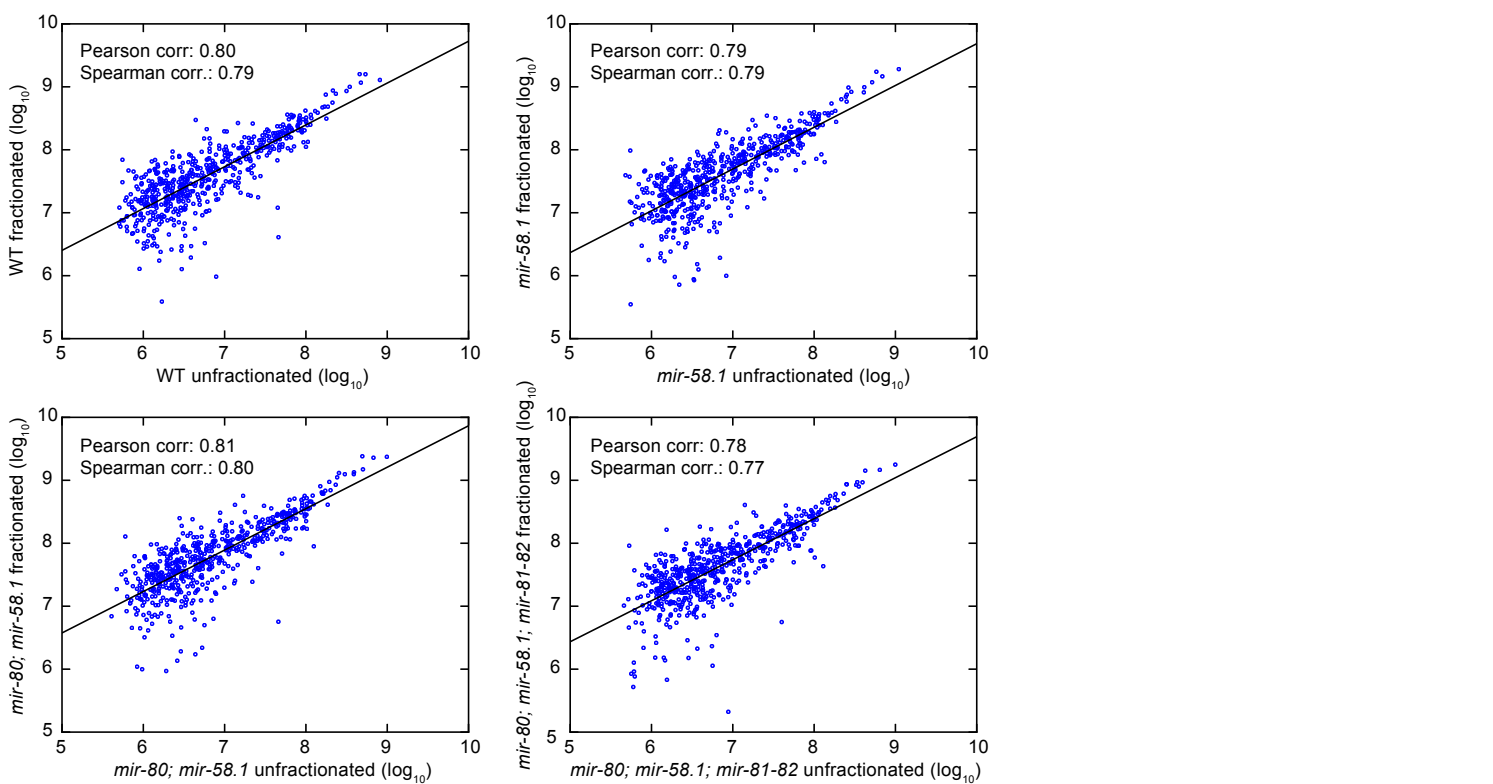
A**B**

Figure S3: Correlation of light labelled peptide intensity (\log_{10}) in fractionated and unfractionated SILAC experiments.
 A, Correlation between three biological replicates of wild-type, *mir-58.1*, *mir-80*; *mir-58.1* and *mir-80*; *mir-58.1*; *mir-81-82* mutant samples measured in unfractionated SILAC experiment. B, Correlation between the average light labelled peptide intensity (\log_{10}) in SILAC unfractionated and SILAC fractionated experiments. Intensity corresponds to the summed up extracted ion current of the isotopic cluster linked to the light label partner (Cox and Mann 2008). Identical protein groups were compared to each other. Pearson and Spearman correlation coefficient are indicated.

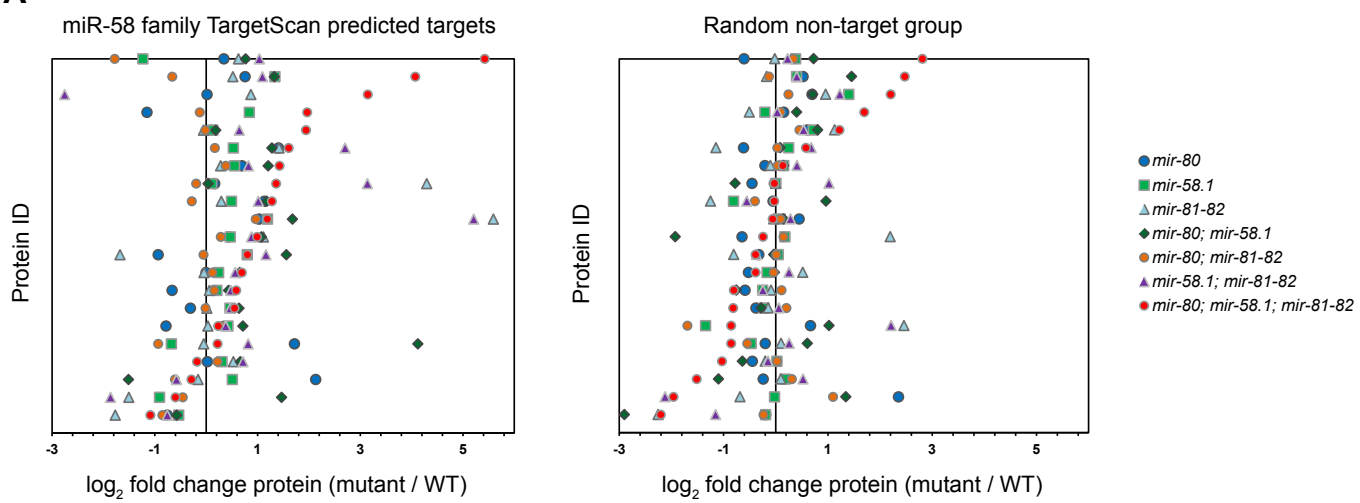
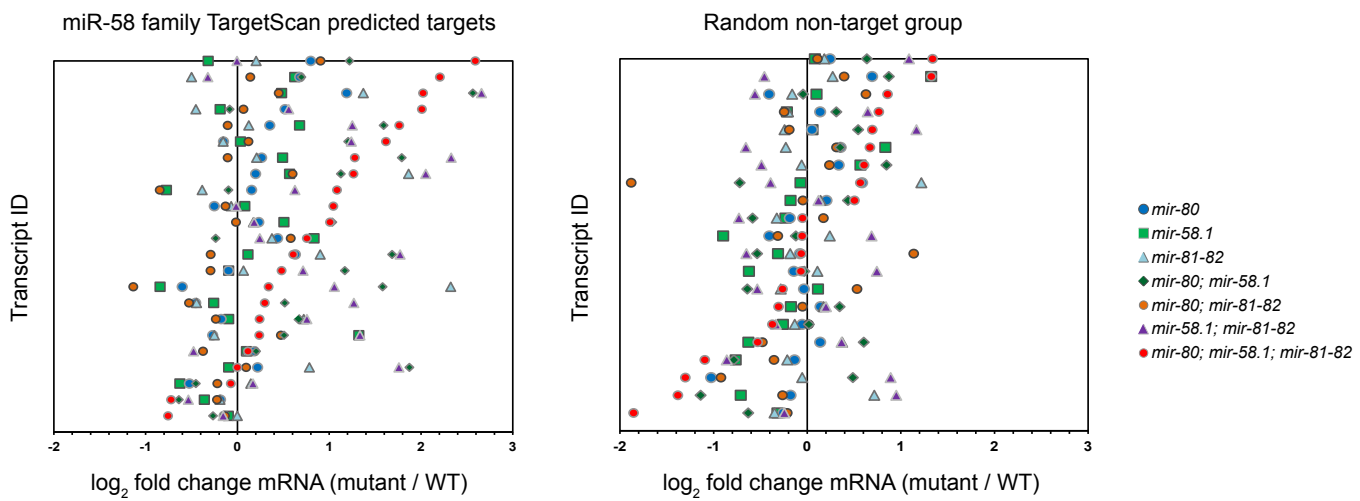
A**B**

Figure S4: Effect of miR-58 family member mutations on target protein and mRNA abundance.

A, Differential expression of 22 TargetScan predicted target proteins and 22 Random control proteins in all combinations of available miR-58 family mutants quantified by SRM. Protein ID indicates a specific protein quantified in different mutants relative to wild-type. Proteins are sorted according to increasing upregulation in the *mir-80; mir-58.1; mir-81-82* quadruple mutant. TargetScan predicted targets are in general shifting towards higher differential expression with each miR-58 family mutation introduced compared to the control random group. B, Differential transcript expression of the same group of targets and non-targets as in A) quantified by qRT-PCR.

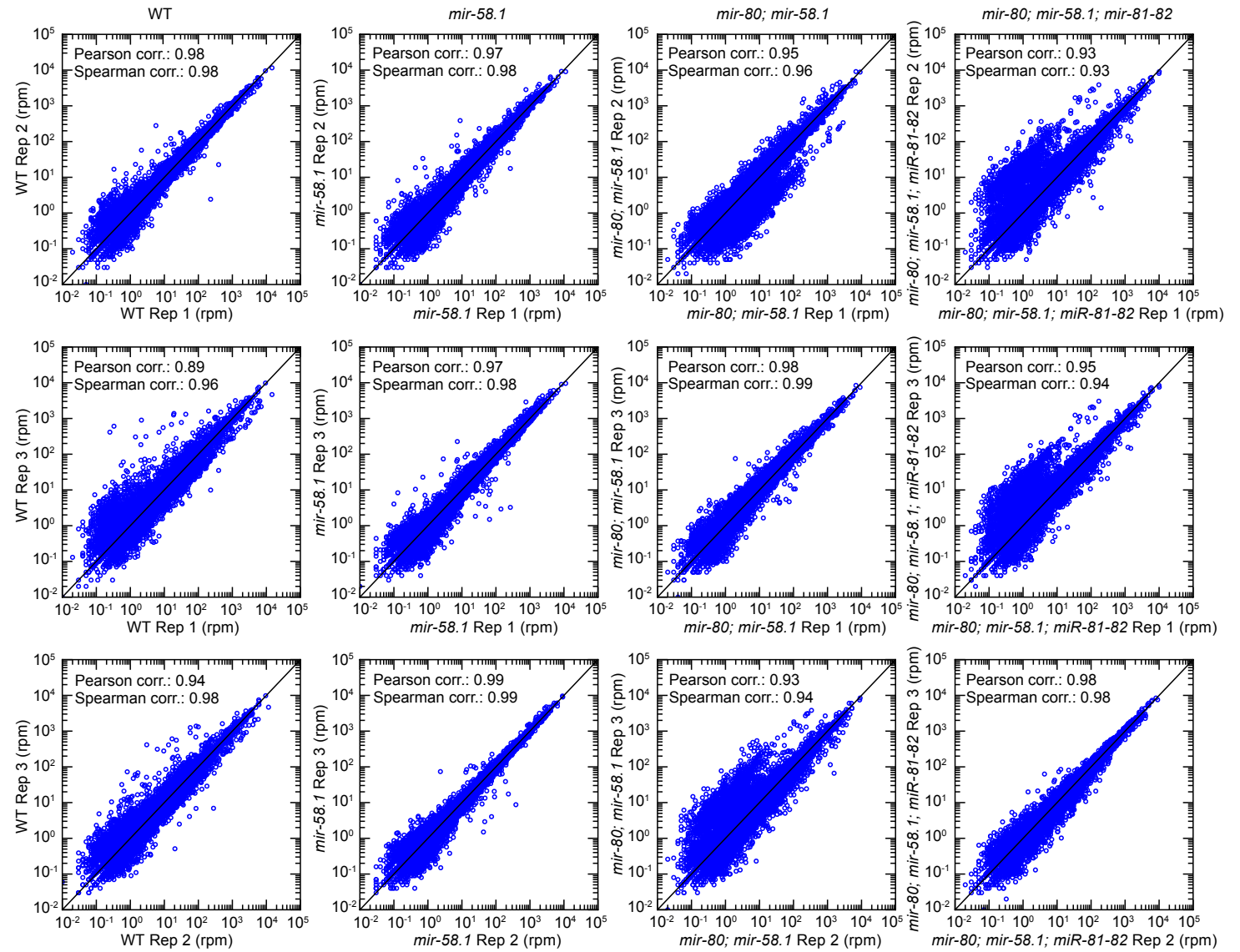


Figure S5: mRNA abundance correlation between three biological replicates of wild-type, *mir-58.1*, *mir-80; mir-58.1* and *mir-80; mir-58.1; mir-81-82* mutant samples quantified by RNA-sequencing.

The abundance is expressed in reads per million (RPM). Pearson and Spearman correlation coefficient are indicated.

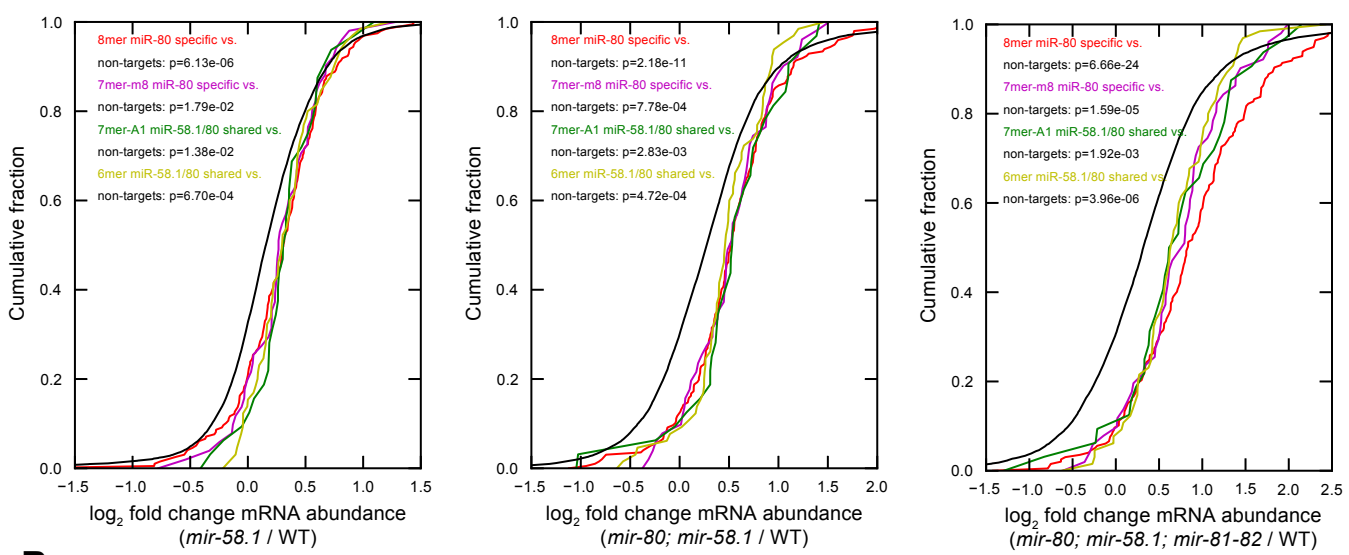
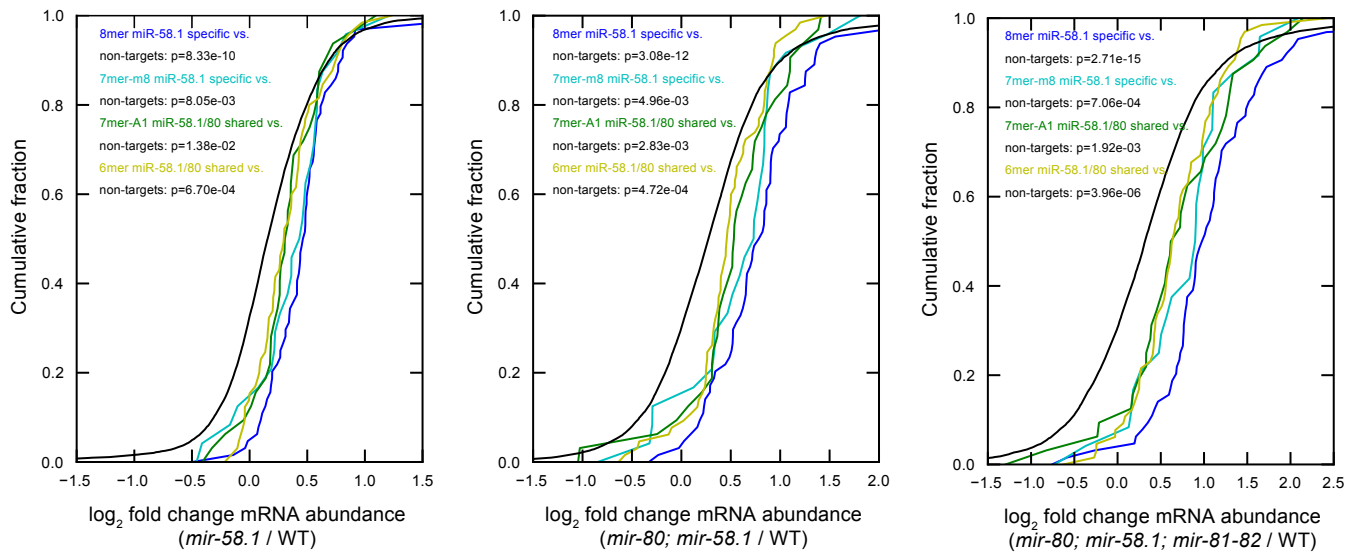
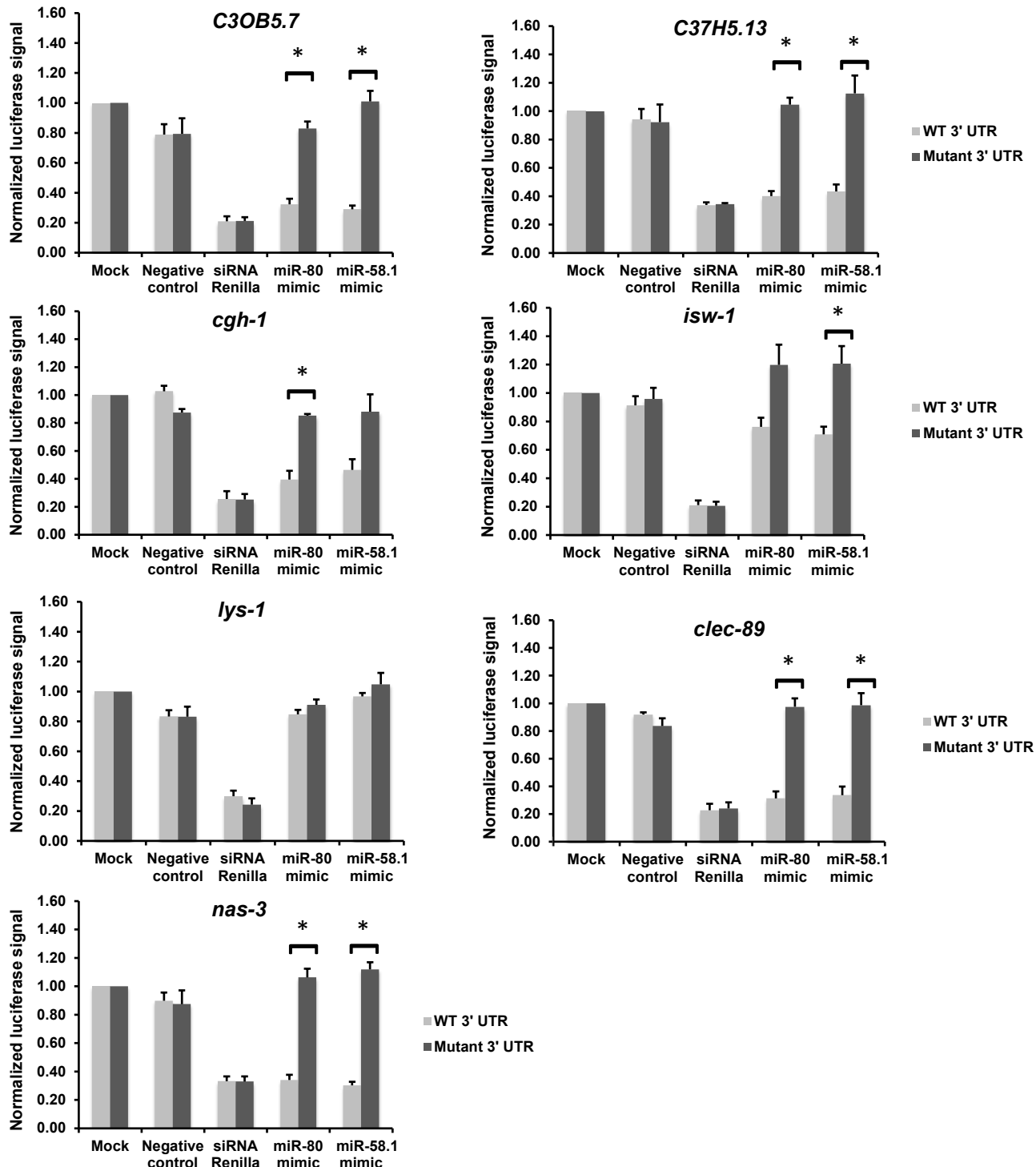
A**B**

Figure S6: Cumulative distributions of \log_2 fold changes in mRNA abundance (miR-58 mutant / WT) of groups of TargetScan predicted miR-58 targets containing different seed matches: 8mer, 7mer-m8, 7mer-A1 and 6mer match for miR-80-specific (A) and miR-58.1 specific targets (B).

P-values were calculated using Kolmogorov-Smirnov (KS) test comparing the fold change distributions (\log_2) of targets with 8-mer, 7mer-m8, 7mer-A1 sites and 6mer sites to non-targets (no seed).

A

Gene name	\log_2 fold change protein (<i>mir-58.1</i> / WT)	\log_2 fold change protein (<i>mir-80; mir-58.1</i> / WT)	\log_2 fold change protein (<i>mir-80; mir-58; mir-81-82</i> / WT)	Protein quantification method	\log_2 fold change mRNA (<i>mir-58.1</i> / WT)	\log_2 fold change mRNA (<i>mir-80; mir-58.1</i> / WT)	\log_2 fold change mRNA (<i>mir-80; mir-58.1; mir-81-82</i> / WT)	3'UTR length (bp)	# of sites	TargetScan predicted specificity
<i>C30B5.7</i>	-1.24	0.76	5.38	SRM	0.86	0.34	0.78	213	1	miR-58.1/80/81/82
<i>C37H5.13</i>	0.37	1.12	1.44	SILAC fr.	0.30	1.03	1.27	165	1	miR-58.1/80/81/82
<i>cgh-1</i>	0.09	0.28	0.33	SILAC unfr.	-0.17	0.98	0.97	988	2	miR-58.1/80/81/82
<i>isw-1</i>	0.47	1.07	0.95	SRM	0.44	1.12	1.38	222	2	miR-58.1/80/81/82
<i>lys-1</i>	0.63	0.95	1.33	SILAC unfr.	0.61	1.67	2.21	141	1	miR-80/81/82
<i>clec-89</i>	NA	NA	NA	NA	0.67	2.57	3.10	134	2	miR-58.1/80/81/82
<i>nas-3</i>	NA	NA	NA	NA	1.44	1.76	3.58	187	1	miR-58.1/80/81/82

B**Figure S7: miR-58.1 and miR-80 mimic suppress miR-58 family targets, but not their miR-58 binding site deleted forms.**

A, Targets chosen for the dual luciferase assay. B, miR-58.1 or miR-80 mimics suppressed six out of seven target 3'UTR reporter constructs in HeLa cells. Sites complementary to the miR-58.1/80 seed were deleted in the mutated 3'UTR. 9 nM concentrations of negative control small interfering (si)RNA (siCON), miR-58.1 and miR-80 mimics, and siRen were transfected into HeLa cells. Selected 3'UTR plasmids were transfected 24 h later at 20 ng per well. Three biological and technical replicates were measured. *, p<0.05, paired t-test: WT vs. mutant 3'UTR.

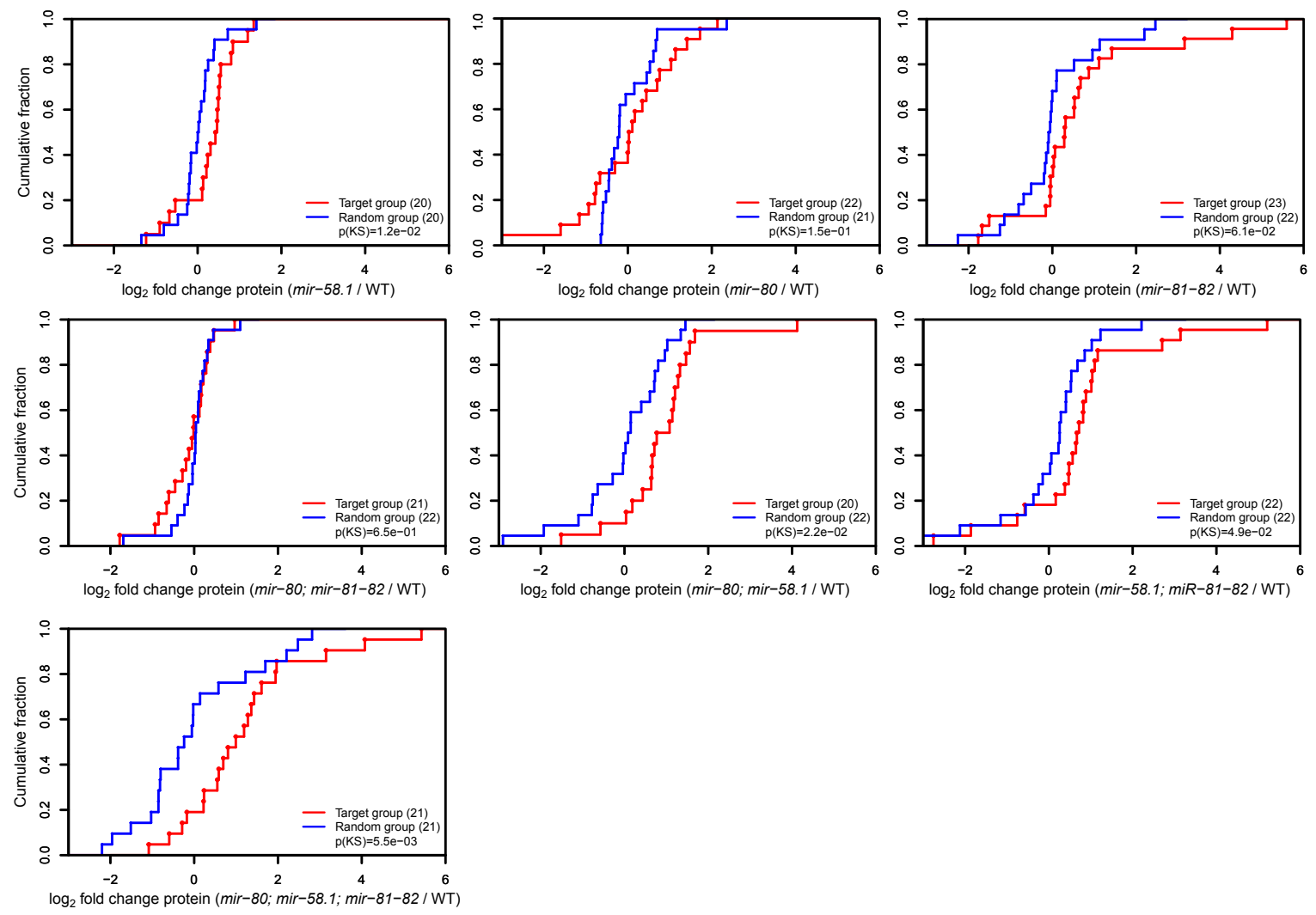


Figure S8: Mutations in miR-58 family members cause additive abundance shifts of the group of target proteins.

Cumulative distributions of \log_2 protein fold changes of 24 TargetScan predicted targets and a control group of 22 random proteins in different miR-58 family mutants and wild-type (measured by selected reaction monitoring). P-values were calculated using Kolmogorov-Smirnov (KS) test comparing the fold change distributions (\log_2) of targets and non-targets.

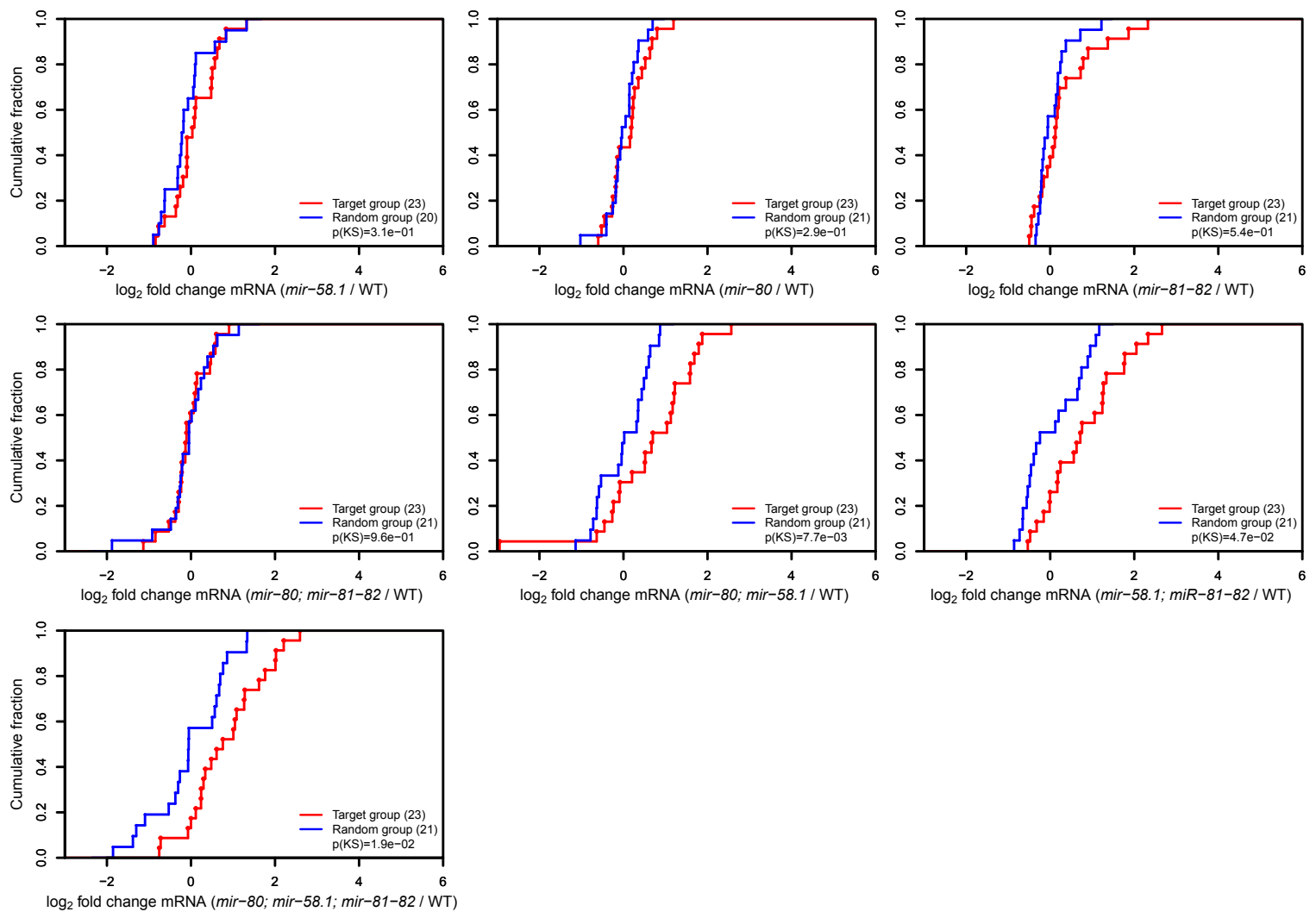


Figure S9: Mutations in multiple, but not single miR-58 family members affect target RNA abundance.

Cumulative distributions of \log_2 mRNA fold changes of 24 TargetScan predicted targets and a control group of 22 random non-targets (as in Fig. S4) in different miR-58 family mutants and wild-type (measured by quantitative RT-PCR). P-values were calculated using Kolmogorov-Smirnov (KS) test comparing the fold change distributions (\log_2) of targets and non-targets.

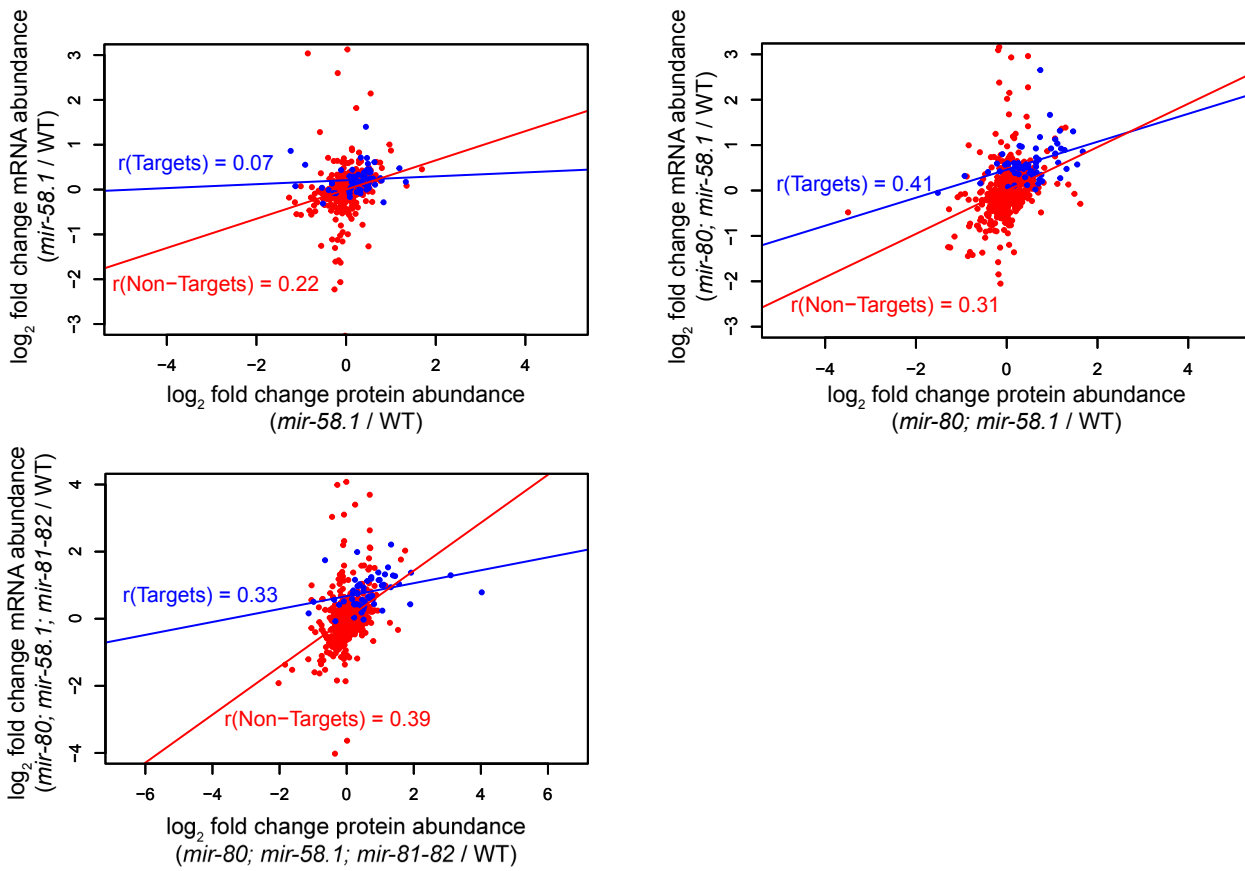


Figure S10: Comparison of protein and RNA changes in miR-58 family mutants.

Targets in *mir-58.1* mutant show no correlation between protein and RNA abundance changes, whereas targets in *mir-80; mir-58.1* and *mir-80; mir-58.1; mir-81-82* show strong positive and moderate positive correlation, respectively. A group of 518 non-targets was used as a control dataset. The Pearson's product moment correlation coefficient of target and non-target group is indicated.

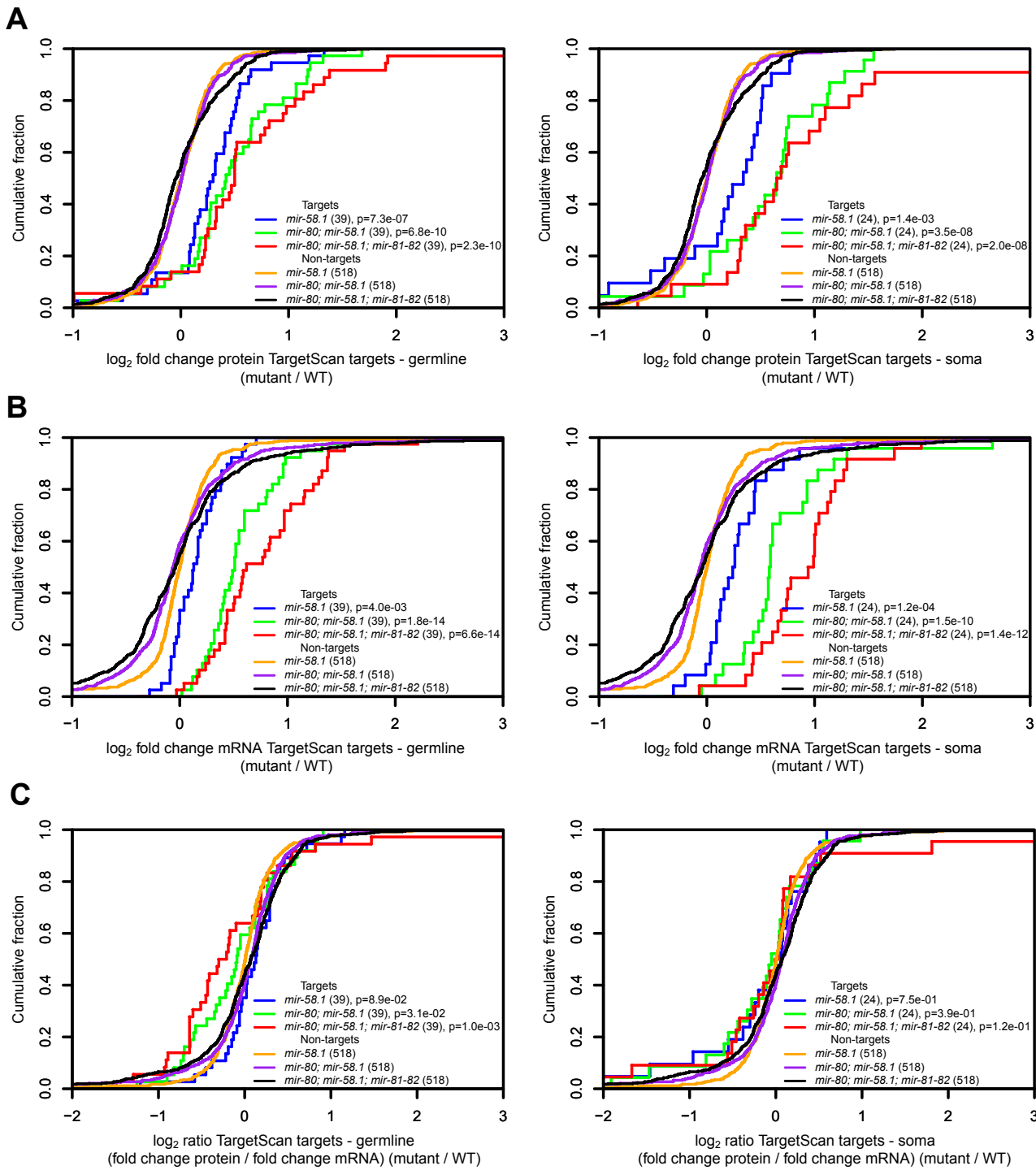


Figure S11: Comparison of quantified miR-58 predicted TargetScan target protein abundances, mRNA abundances and translation efficiencies for germline-expressed and soma-expressed transcripts in different miR-58 family mutants.

Cumulative distributions of \log_2 fold protein expression (A), mRNA expression (B) and translation efficiency (C) changes of the 39 germline- and 24 soma-expressed TargetScan-predicted miR-58 targets in the *mir-58.1* single, *mir-80; mir-58.1* double and *mir-80; mir-58.1; mir-81-82* quadruple mutants relative to WT. Germline expressed genes were extracted from the SAGE library of hand dissected gonads (Wang et al. 2009) and the rest are considered soma-expressed genes. Quantified TargetScan predicted targets identified in SRM, fractionated SILAC and unfractionated SILAC were compared to a group of 518 non-targets identified in unfractionated SILAC measurements for which we also had transcript abundance data. P-values were calculated using Kolmogorov-Smirnov (KS) test comparing the fold change distributions (\log_2) of targets and non-targets.

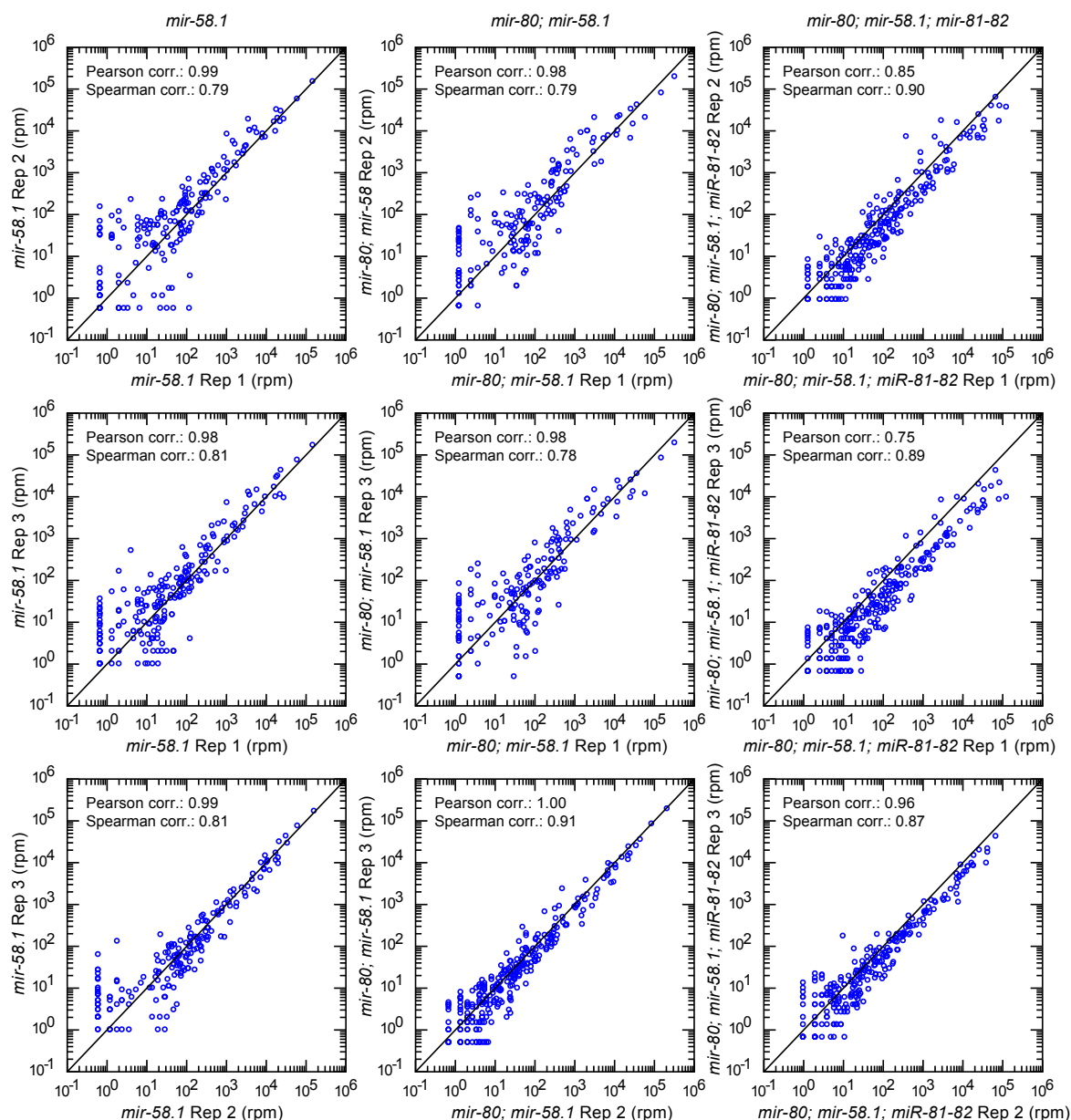


Figure S12: miRNA abundance correlation between three biological replicates of wild-type, *mir-58.1*, *mir-80*; *mir-58.1* and *mir-80*; *mir-58.1*; *mir-81-82* mutant samples quantified by small RNA-seq.

The abundance is expressed in reads per million (RPM). Pearson and Spearman correlation coefficient are indicated.

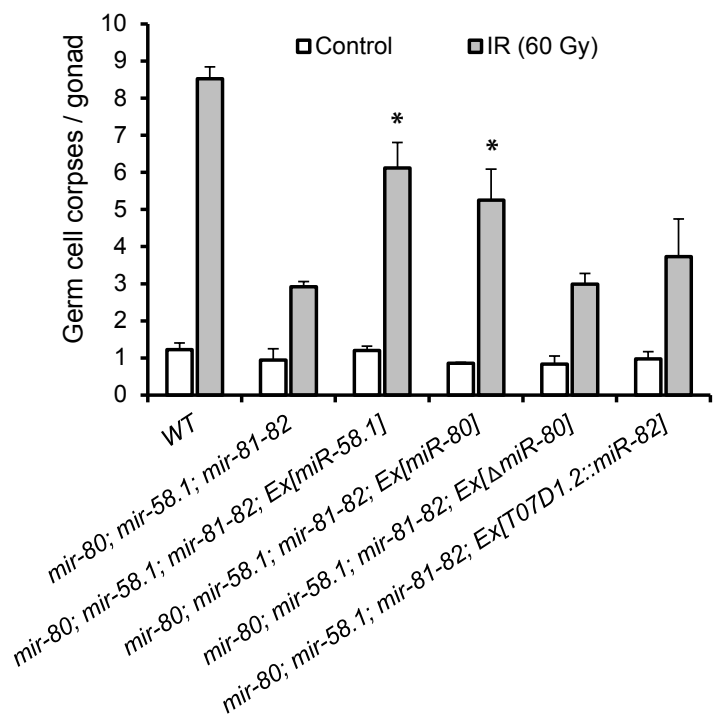


Figure S13: miR-58.1 and miR-80 transgenes partially restore IR-induced apoptosis in the miR-58 family mutant.

Error bars represent the standard error of the mean from three biological replicates (25 worms per experiment). *, p<0.001, paired t-test: transgene vs. miR-58 family mutant.

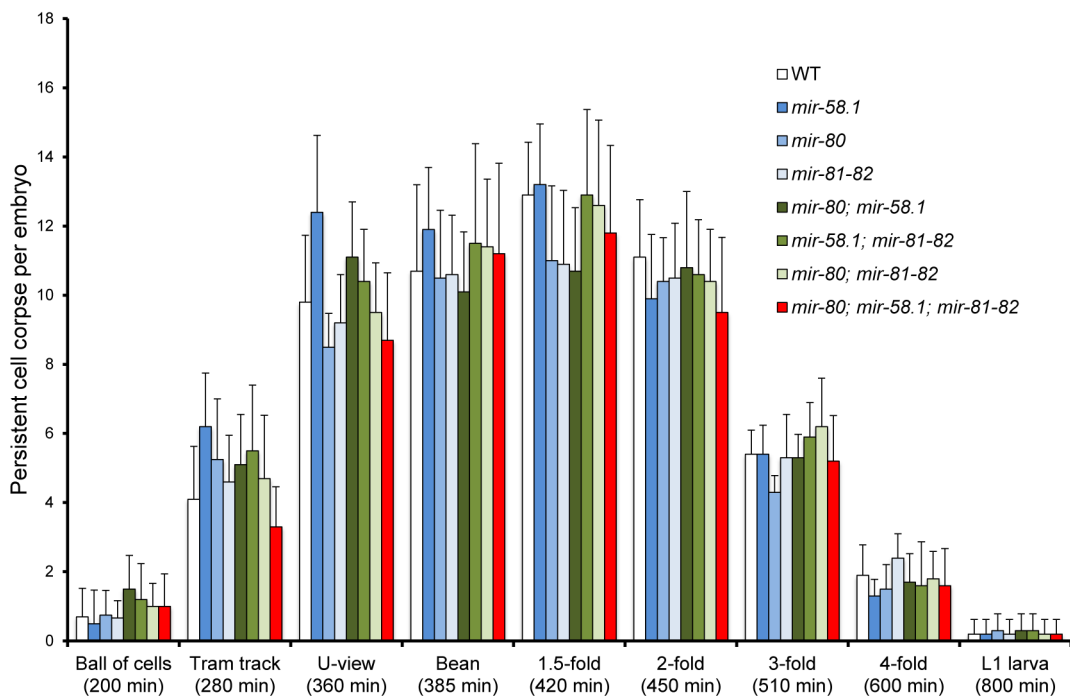


Figure S14: Developmental cell death is not affected in miR-58 family mutants.

Cell corpses were scored in various stages of embryonic development. Time post-fertilization is stated in parentheses. Error bars represent the standard deviation (n=25 animals).